Arctic Ocean sea ice drift origin derived from artificial radionuclides

P. Cámara-Mor [a,*], P. Masqué [a,b], J. Garcia-Orellana [a,b,c], J.K. Cochran [c], J.L. Mas [d], E. Chamizo [e], C. Hanfland [f]

[a] Institut de Ciència i Tecnologia Ambientals, Universitat Autònoma de Barcelona, E-08193. Bellaterra, Spain
[b] Dpt. de Física, Universitat Autònoma de Barcelona, E-08193. Bellaterra, Spain
[c] School of Marine & Atmospheric Sciences, Stony Brook University, Stony Brook, NY 11794-5000, USA
[d] Dpto. de Física Aplicada, Universidad de Sevilla, 41012, Seville. Spain
[e] Centro Nacional de Aceleradores (CNA), Avd. Thomas Alva Edison 7, Isla de la Cartuja, E-41092, Seville, Spain
[f] Alfred Wegener Institute for Polar and Marine Research, Am Handelshafen 12, D-27570 Bremerhaven, Germany

ARTICLE INFO

Article history:
Received 11 August 2009
Received in revised form 22 March 2010
Accepted 25 March 2010

Keywords:
Arctic Ocean
Sea-ice sediments
^{137}Cs
^{239,240}Pu
^{240}Pu/^{239}Pu atom ratio
Sea ice origin
Geotraces

ABSTRACT

Since the 1950s, nuclear weapon testing and releases from the nuclear industry have introduced anthropogenic radionuclides into the sea, and in many instances their ultimate fate are the bottom sediments. The Arctic Ocean is one of the most polluted in this respect, because, in addition to global fallout, it is impacted by regional fallout from nuclear weapon testing, and indirectly by releases from nuclear reprocessing facilities and nuclear accidents. Sea-ice formed in the shallow continental shelves incorporate sediments with variable concentrations of anthropogenic radionuclides that are transported through the Arctic Ocean and are finally released in the melting areas. In this work, we present the results of anthropogenic radionuclide analyses of sea-ice sediments (SIS) collected on five cruises from different Arctic regions and combine them with a database including prior measurements of these radionuclides in SIS. The distribution of ^{137}Cs and ^{239,240}Pu activities and the ^{240}Pu/^{239}Pu atom ratio in SIS showed geographical differences, in agreement with the two main sea ice drift patterns derived from the mean field of sea-ice motion, the Transpolar Drift and Beaufort Gyre, with the Fram Strait as the main ablation area. A direct comparison of data measured in SIS samples against those reported for the potential source regions permits identification of the regions from which sea ice incorporates sediments. The ^{240}Pu/^{239}Pu atom ratio in SIS may be used to discern the origin of sea ice from the Kara–Laptev Sea and the Alaskan shelf. However, if the ^{240}Pu/^{239}Pu atom ratio is similar to global fallout, it does not provide a unique diagnostic indicator of the source area, and in such cases, the source of SIS can be constrained with a combination of the ^{137}Cs and ^{239,240}Pu activities. Therefore, these anthropogenic radionuclides can be used in many instances to determine the geographical source area of sea-ice.

1. Introduction

The Arctic Ocean is often considered as a pristine area, but it cannot avoid the effect of industrialization and development. It is thus subject to inputs of contaminants such as heavy metals, persistent organic pollutants and anthropogenic radionuclides (MacDonald et al., 2005). Since the 1950s, anthropogenic radionuclides such as ^{137}Cs and the Pu isotopes (e.g. ^{239}Pu, ^{240}Pu) have been introduced and distributed worldwide, including the Arctic Ocean. During the past two decades numerous national and international programs have been carried out to study the distribution, sources, transport and behaviour of artificial radionuclides in the Arctic Ocean (e.g. Yablokov et al., 1993; JRNEG, 1994, 1996; AMAP, 1998). The main source of anthropogenic radionuclides in the Arctic Ocean has been global stratospheric fallout (JRNEG, 1996; Oughton et al., 2004). However, secondary sources have also been significant. Regional or tropospheric fallout resulted from nuclear weapons tests carried out by the former Soviet Union (FSU) at the Novaya Zemlya archipelago (85 atmospheric, 3 underwater, 2 surface water tests between 1955 and 1990) and at Semipalatinsk (86 atmospheric, 30 ground surface and 340 underground tests) (Salbu, 2001). Nuclear wastes from reprocessing facilities also contributed to the overall inventories of ^{137}Cs and Pu in Arctic Ocean, including discharges from Sellafield (UK) and, to a lesser extent, from La Hague (France) (Holm, 1994; Aarkrog, 2003). Also, the Ob and Yenisey rivers contribute terrestrial run-off which has received radionuclides from weapons testing at Semipalatinsk and discharges from nuclear facilities located near or on the rivers (Tomsk-7 and Mayak) (e.g. JRNEG, 1994, 1996, Oughton et al. 1999; Smith et al., 1995). For example, it has been documented the release of about 100 TBq of liquid waste from Mayak, including about 2 TBq of alpha emitters, to the Techa River during 1948–1951 (Christensen et al., 1997; Vorobiova et al., 1999). Other reprocessing plants such as Krasnoyarsk-26 discharged about 30 to 100 TBq of ^{137}Cs into the Kara Sea between 1958 and 1993 (Vakulovsky et al., 1995). Finally, the FSU also dumped liquid and solid radioactive

* Corresponding author. Tel.: +34 93 581 11 91; fax: +34 93 581 21 55.
E-mail address: patricia.camara@uab.es (P. Cámara-Mor).

0048-9697/$ – see front matter doi:10.1016/j.scitotenv.2010.03.041

wastes into the Barents and Kara Seas between 1960 and 1991. Overall, the total amount of radioactive wastes dumped in the Arctic Ocean was estimated by the IAEA (1998) to be of approximately 37 PBq. Nuclear accidents have also contributed artificial radionuclides into the Arctic environment, such as those occurred in Kyshtym in 1957 and in Tromsk-7 in 1993 (Kabakchi et al., 1995; Waters et al., 1999).

Once radionuclides are introduced into the sea they can be scavenged from seawater by particulate matter and be eventually deposited in sediments in the bottom floor (e.g. Livingston and Bowen, 1979; Baxter et al., 1995; Aarkrog, 2003). In the Arctic Ocean, several studies have focussed on studying the distributions of ^{137}Cs and ^{239,240}Pu and the ^{240}Pu/^{239}Pu atom ratio (which is a useful indicator of Pu origin —Masqué et al., 2003—) in bottom sediments from the central Arctic Basin (Huh et al., 1997; Cooper et al., 2000) and from the Fram Strait (Masqué et al., 2003). However, most studies have paid attention to the continental shelves, particularly along the Siberian shelves, as they are the most affected areas by introduction of artificial radionuclides (e.g. Baskaran et al., 1996, 2000; Cochran et al., 2000; Smith et al., 2000).

The Arctic continental shelves, specially in the Siberian area, are one of the main sources of sea ice (Fig. 1). During sea ice formation in these shallow areas, sediments and suspended particles are mainly incorporated by suspension freezing into the ice. As a result, sea ice can contain a significant amount of sediments (sea-ice sediments, SIS) ranging from a few grams to tens of kilograms per cubic meter (Nürnberg et al., 1994). Although aeolian deposition onto the ice is also possible, field evidence for such a process is very sparse and its deposition rate on the central Arctic ice cover appears to be several orders of magnitude less than the other contributions to SIS loads (Pfirman et al., 1989, 1990; Nürnberg et al., 1994). Thus in general it is assumed that “dirty ice” (ice with high concentrations of sediment) has been formed on shallow shelves.

The particulate matter and the associated chemical species contained in sea ice are transported from continental shelf areas to the central Arctic basin in association with the physical circulation. The mean sea-ice drift patterns are controlled by the Transpolar Drift (TPD) over the Eurasian Basin and the anticyclonic Beaufort Gyre in the Canada Basin (Thorndike, 1986). Sea ice formed over the western Siberian shelves is carried by the TPD with a transit time of 2–4 years to the Fram Strait (Thorndike and Colony, 1982). Sea ice which rotates in the Beaufort Gyre may circulate there for ~5 to 15 years, and is generally thought to be formed in the Beaufort, Chukchi and East Siberian Seas, although it is also possible to find sea ice from the TPD in the Beaufort Gyre (Thorndike, 1986). As sea ice reaches ablation areas such as the Fram Strait and, to a lesser degree, also along the central Arctic Ocean or in the Canadian archipelago, it melts and releases the entrained particulate matter to the surface water (Pfirman et al., 1997; Rigor et al., 2002). Hence, sea ice has been identified as playing a potentially important role in the redistribution and transport of particulate matter and chemical species in the Arctic Ocean (e.g. Nürnberg et al., 1994; Landa et al., 1998; Masqué et al., 2003).

In this work we use new and published data on concentrations of ^{137}Cs, ^{239,240}Pu and the ^{240}Pu/^{239}Pu atom ratio in SIS in the Arctic

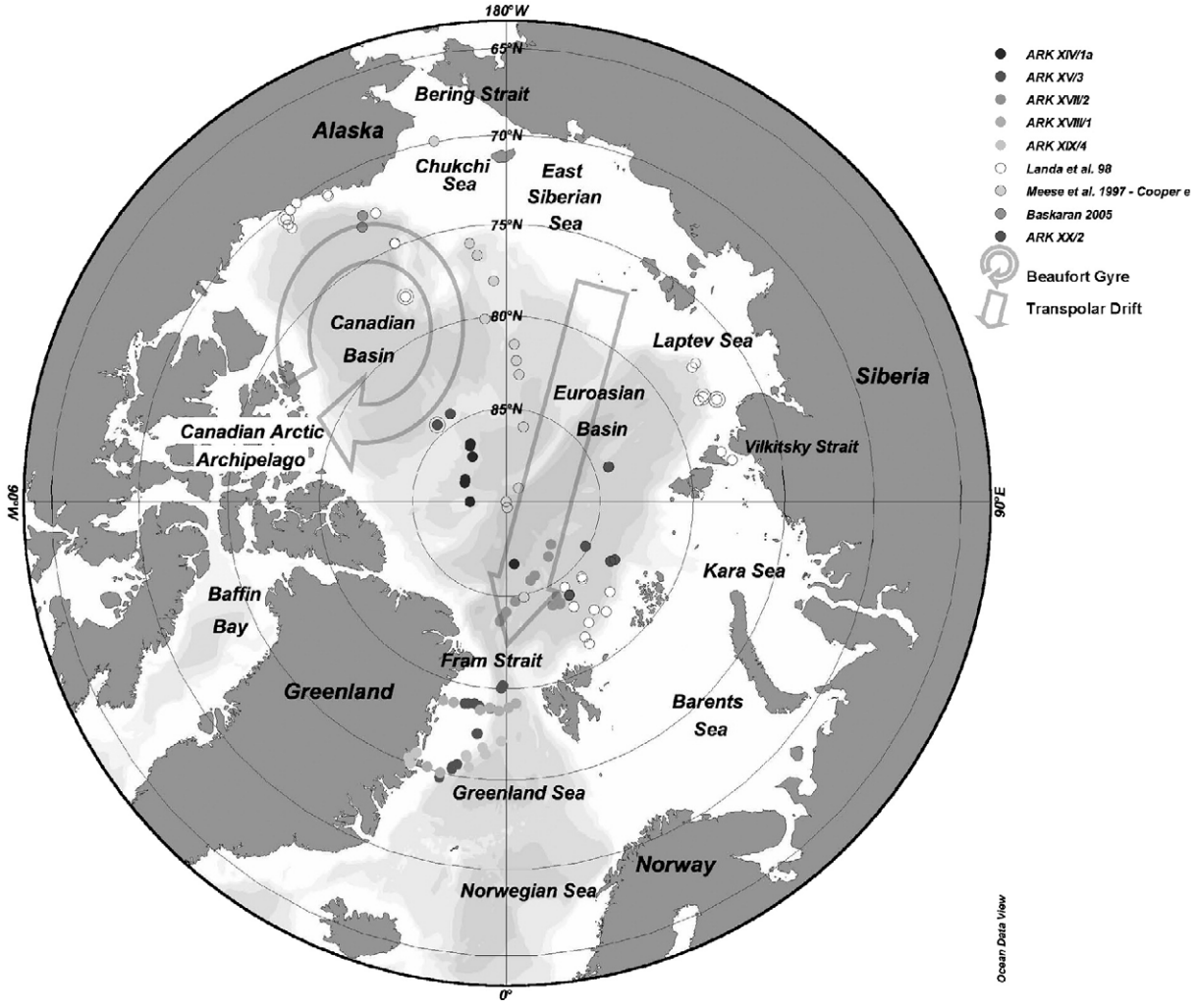

Fig. 1. Arctic Ocean topography and sea ice drift pattern.

Ocean to assess the possible origin of the sea ice which forms the ice pack.

2. Materials and methods

2.1. Sampling

A total of 63 SIS samples were collected during several cruises of R/V Polarstern (Table 1). Samples were recovered from annual or multi-year sea ice and icebergs from the central Arctic Ocean, the Nansen Basin and the Fram Strait. Approximately 10 to 200 g of SIS were collected from the upper surface of the ice floes, from ridges and from cryoconites holes (small holes produced by aggregation of particles in the surface ice by absorption of solar energy) by scraping with stain-steel shovels or/an ice-hammer in order to obtain blocs of turbid sea ice. Once onboard, sea-ice samples were thawed and SIS were isolated from the supernatant liquid by careful decantation. Afterwards, SIS samples were kept frozen and stored in plastic bags until their analysis in the laboratory. Before radionuclide analysis, all samples were dried in an oven at 60 °C and ground to a powder.

2.2. Radiometric analysis

2.2.1. ^{137}Cs

The activity of ^{137}Cs ($T_{1/2}=30.1$ y) was determined by gamma spectrometry using a Ge detector at the Universitat Autònoma de Barcelona (UAB, Spain) and at Stony Brook University. Dry samples were hermetically sealed in containers with well known geometries (plastic vials at UAB and aluminium cans at Stony Brook University). In both cases, ^{137}Cs was determined through its gamma emission at 661.6 keV. Counting times were typically about 2 days, with uncertainties <10%. All ^{137}Cs activities were decay-corrected to first of September 2007 in order to make all data comparable.

2.2.2. Plutonium isotopes

Concentrations of ^{239}Pu ($T_{1/2}=24110$ y) and ^{240}Pu ($T_{1/2}=6560$ y) and the $^{240}Pu/^{239}Pu$ atom ratios in SIS samples collected during ARK XIV/1a and ARK XVII/2 cruises were measured by using a Finningan ELEMENT magnetic-sector inductively coupled plasma mass spectrometer (MS-ICPMS) at Woods Hole Oceanographic Institution, Massachusetts. These samples were analysed following the procedure described by Masqué et al. (2003) based upon the methods developed by Buesseler (1986) and Kenna (2002). Briefly, a known amount of ^{242}Pu was added as an internal yield tracer to 2–25 g of sample which were incinerated at 550 °C for 24 h. The ashes were digested with 8 N HNO_3. Pu was separated by ion exchange, and samples underwent several steps in order to obtain an adequate separation from other transuranic nuclides. Pu was eluted from the final ion exchange column with 10% HNO_3–1% HF and the solution was evaporated to 1 mL.

In the case of SIS samples collected during ARK XVIII/1, ARK XIX/4 and ARK XXII/2 cruises, concentrations of ^{239}Pu, ^{240}Pu and the $^{240}Pu/^{239}Pu$ atom ratios were determined by accelerator mass spectrometry (AMS) at the Centro Nacional de Aceleradores (CNA, Sevilla). Details concerning the chemical procedure and the AMS measurement technique can be found in Chamizo et al. (2008a,b). Briefly, about 2 g of dried SIS were spiked with 10 pg of ^{242}Pu as a yield monitor, ashed at 600 °C for 6 h and acid digested with HNO_3 (65%), H_2O_2 (30%) and HF (40%). The supernatant was separated from the residue after centrifuging the solution at 4000 rpm. Prior to ion exchange purification, the solution was prepared to contain Pu only in the IV oxidation state by adding 0.18 g of $NaNO_3$. Ion exchange separation was performed with TEVA-columns. The Pu fraction was isolated from the other actinides by washing the column with 6 M HCl to remove Th and 8 M HNO_3 to remove U. Pu was eluted with 0.002 M HF and 0.02 M HNO_3 and the eluate was evaporated to 3 mL and transferred to plastic vials for storage prior to measurement by AMS-CNA.

All Pu concentrations and isotope ratios were blank corrected. The measured atom concentrations of ^{239}Pu and ^{240}Pu have been converted into activities and added to be expressed as $^{239,240}Pu$ in order to facilitate comparison with previous works.

Table 1
Data on sampling cruises on board RV Polarstern, year, areas of study and number of SIS samples collected.

Name cruise	Year	Expedition area	Number of samples
ARK XIV/1a	July 1998	Central Arctic Basin	12
ARK XV II/2	August-September 2001	Nansen Basin	13
ARK XVIII/1	July-August 2002	Fram Strait	10
ARK XIX/4	Augost-September 2003	Fram Strait	12
ARK XXII/2	July-October 2007	Along Transporlar Drift	16

3. Results

The specific activities of artificial radionuclides (^{137}Cs and $^{239,240}Pu$) and the $^{240}Pu/^{239}Pu$ atom ratios in sea-ice sediments are summarized in Table 2. The ^{137}Cs activities showed a large variability, ranging from 1.8 to $4\cdot10^3$ Bq kg^{-1}, although only 5% of the samples contained ^{137}Cs activities higher than 38 Bq kg^{-1}. Outliers have been identified by box plot analysis, based upon inter-quartile differences. Median values were used since the data do not follow a normal distribution. Excluding these samples, the average ^{137}Cs activity was 9.1 ± 7.4 Bq kg^{-1} ($n=51$). The highest ^{137}Cs specific activity, $4\cdot10^3$ Bq kg^{-1}, was determined in sediments collected from an iceberg sampled from the waters near Franz Josef Land. This value is even greater than concentrations of ^{137}Cs reported by Cota et al. (2006) in sea-ice sediments from the Canadian Archipelago ($\sim2.5\cdot10^3$ Bq kg^{-1}).

The $^{239,240}Pu$ specific activities also showed considerable variability, varying up to four orders of magnitude from 0.018 to 31.8 Bq kg^{-1}, although most of the samples (95%) had $^{240,239}Pu$ activities <1.4 Bq kg^{-1}. Excluding the samples with concentrations >1.4 Bq kg^{-1}, activities of $^{240,239}Pu$ in SIS averaged 0.32 ± 0.25 Bq kg^{-1} ($n=45$). The samples with $^{240,239}Pu$ concentrations >1.4 Bq kg^{-1} were collected throughout the Nansen Basin, although mainly in the western part of the Fram Strait. In general, high $^{240,239}Pu$ concentrations are also characterised by high ^{137}Cs concentrations (>45 Bq kg^{-1}) (Table 2).

The $^{240}Pu/^{239}Pu$ atom ratios ranged from 0.118 to 0.253 (Table 2). Most of the $^{240}Pu/^{239}Pu$ atom ratios in SIS samples were consistent with the atom ratio characteristic of global fallout (0.183 ± 0.009) measured in sediment samples collected at 70ºN by Efurd et al. (2005). 25% of the samples had $^{240}Pu/^{239}Pu$ atom ratios lower than 0.174, and they had been mainly collected in the Fram Strait and north of Franz Josef Land. Another 25% of the samples had $^{240}Pu/^{239}Pu$ atom ratios >0.195, ranging up to 0.253, and in most cases were also collected in the Fram Strait. Samples with relatively low $^{240}Pu/^{239}Pu$ atom ratios (<0.174) also generally had relatively high concentrations of $^{240,239}Pu$ (>1 Bq kg^{-1}) and ^{137}Cs (up to 45 Bq kg^{-1}), except for samples 15, 228, 270-2 and PS70/3, which were collected in the Eurasian Basin. The samples with low $^{240}Pu/^{239}Pu$ atom ratios and high ^{137}Cs concentrations were collected in the Fram Strait and the Nansen Basin during summer in 2001 and 2002.

4. Discussion

In order to study the geographical distributions of ^{137}Cs and $^{239,240}Pu$ concentrations and $^{240}Pu/^{239}Pu$ atom ratios in SIS along the Arctic Ocean it is necessary to consider our data in the context of previous results such as those by Meese et al. (1997), Landa et al.

Table 2
Specific activities ($\pm 1\sigma$) of ^{137}Cs, ^{239,240}Pu and ^{240}Pu/^{239}Pu atom ratios in sea-ice sediments collected from the Arctic Ocean. n.m.: not measured.

Code	Date	Lat N	Long E	^{137}Cs (Bq kg^{-1})	^{239,240}Pu (Bq kg^{-1})	^{240}Pu/^{239}Pu
ARK XIV/2 — Central Arctic Basin						
5	08-jul-98	86.658	7.690	13.3 ± 0.7	0.26 ± 0.02	0.20 ± 0.03
8	10-jul-98	88.073	−89.887	9.9 ± 0.5	0.06 ± 0.03	n.m
11	12-jul-98	87.572	−115.094	13.2 ± 0.9	0.141 ± 0.008	0.19 ± 0.02
12	12-jul-98	87.578	−116.606	15.5 ± 0.9	0.183 ± 0.011	0.19 ± 0.02
14	12-jul-98	87.520	−118.825	14.3 ± 0.8	0.09 ± 0.02	n.m
15	13-jul-98	86.992	−143.379	8.3 ± 0.6	0.096 ± 0.009	0.17 ± 0.04
17	13-jul-98	86.457	−147.240	8.0 ± 0.9	0.29 ± 0.03	0.19 ± 0.04
18	14-jul-98	86.373	−148.478	12.9 ± 0.7	0.109 ± 0.006	0.18 ± 0.02
23	18-jul-98	85.673	−176.937	n.m	0.032 ± 0.011	n.m
25	18-jul-98	85.653	−177.862	n.m	0.16 ± 0.05	0.17 ± 0.11
27	21-jul-98	83.560	144.983	n.m	0.084 ± 0.014	0.18 ± 0.06
29	23-jul-98	81.473	145.065	n.m	0.169 ± 0.011	0.17 ± 0.11
ARK XV II/2 — Nansen Basin						
217	05-aug-01	83.950	24.250	3.7 ± 0.3	0.136 ± 0.007	0.18 ± 0.02
218	06-aug-01	85.633	17.313	4.15 ± 0.44	0.083 ± 0.010	n.m
220	08-aug-01	84.667	5.100	14.4 ± 1.1	0.97 ± 0.04	0.184 ± 0.016
222	10-aug-01	84.133	0.017	25.2 ± 1.6	1.23 ± 0.02	0.186 ± 0.008
223	11-aug-01	83.636	−2.975	11.9 ± 0.7	0.474 ± 0.011	0.189 ± 0.009
228	16-aug-01	83.791	−2.199	4.2 ± 0.4	0.211 ± 0.013	0.118 ± 0.019
270-2	27-sep-01	84.289	28.258	14.2 ± 0.8	0.54 ± 0.08	0.17 ± 0.05
270-3	27-sep-01	83.873	28.258	4.3 ± 0.3	0.246 ± 0.005	0.179 ± 0.008
270-4	27-sep-01	83.853	27.855	13.8 ± 1.4	0.94 ± 0.05	0.20 ± 0.02
Iceberg-1	21-aug-01	85.050	11.040	n.m	0.66 ± 0.03	0.18 ± 0.02
Iceberg-2	29-aug-01	86.333	37.767	1.79 ± 0.17	0.021 ± 0.002	0.18 ± 0.04
Iceberg-5	17-sep-01	86.720	46.653	4001.5 ± 77.6	31.9 ± 0.8	0.165 ± 0.009
Iceberg-6	23-sep-01	85.800	21.390	4.2 ± 0.3	0.205 ± 0.008	0.25 ± 0.02
ARK XVIII/1 — Fram Strait						
01-1	30-jul-02	75.123	−16.528	n.m	0.044 ± 0.004	n.m
02-1	30-jul-02	75.009	−13.641	10.1 ± 0.4	0.24 ± 0.09	0.189 ± 0.015
03-1	8-aug-02	79.200	2.672	6.1 ± 0.7	0.223 ± 0.017	0.19 ± 0.03
05-2	12-aug-02	78.967	0.655	6.4 ± 0.5	0.71 ± 0.05	0.210 ± 0.024
06-2	13-aug-02	78.782	−2.002	3.5 ± 0.2	0.70 ± 0.03	0.21 ± 0.02
07-1	14-aug-02	78.943	−4.600	7.7 ± 0.3	0.086 ± 0.005	n.m
08-1	14-aug-02	78.756	−7.113	480.6 ± 2.3	7.69 ± 0.13	0.166 ± 0.007
08-3	14-aug-02	78.756	−7.113	651.7 ± 3.3	9.5 ± 0.4	0.187 ± 0.007
09-1	15-aug-02	78.909	−14.648	4.8 ± 0.5	0.75 ± 0.05	n.m
10-1	15-aug-02	78.844	−17.657	136.3 ± 0.9	2.52 ± 0.10	0.155 ± 0.009
ARK XIX/4 — Fram Strait						
PS64 HELI02-2	15-aug-03	76.380	−4.654	3.9 ± 0.7	0.144 ± 0.008	0.187 ± 0.017
PS64 HELI04-1	16-aug-03	76.750	−5.480	5.4 ± 0.8	0.262 ± 0.017	0.19 ± 0.02
PS64 HELI04-2	16-aug-03	76.747	−5.459	4.2 ± 0.4	0.254 ± 0.012	0.193 ± 0.013
PS64 HELI05-1	20-aug-03	77.150	−1.172	5.6 ± 0.3	0.144 ± 0.011	0.17 ± 0.02
PS64 HELI06-1	20-aug-03	77.150	−1.201	5.6 ± 0.3	0.186 ± 0.015	n.m
PS64 HELI07-1	25-aug-03	75.586	−8.048	4.5 ± 0.6	0.124 ± 0.010	0.16 ± 0.03
PS64 HELI09-2a	29-aug-03	75.013	−20.101	22.4 ± 0.2	0.141 ± 0.012	n.m
PS64 HELI11-1	5-sep-03	76.115	−8.745	4.3 ± 0.6	0.44 ± 0.02	0.175 ± 0.012
PS64 HELI11-3	5-sep-03	76.216	−8.999	126.2 ± 8.4	2.92 ± 0.13	0.143 ± 0.009
PS64-HELI12.2	6-sep-03	75.622	−19.735	23.1 ± 0.2	n.m	n.m
PS64-HELI12.3	6-sep-03	75.261	−20.905	8.7 ± 1.5	n.m	n.m
PS64 HELI14-2a	14-sep-03	73,357	−23.818	n.m	0.018 ± 0.005	n.m
ARK XXII/2 — Along transpolar drift						
PS70/1.1	6-aug-07	83.994	34.026	31.8 ± 1.3	n.m	n.m
PS70/1.3	6-aug-07	83.994	34.026	29.9 ± 2.8	0.78 ± 0.03	0.157 ± 0.006
PS70/2.C.2	6-aug-07	83.993	34.385	29.6 ± 0.9	0.68 ± 0.02	0.177 ± 0.007
PS70/2.D.2	6-aug-07	83.993	34.385	19.2 ± 0.5	0.66 ± 0.02	n.m
PS70/4.1	12-aug-07	83.605	60.3989	4.8 ± 1.0	0.210 ± 0.018	0.21 ± 0.03
PS70/4.2	12-aug-07	83.605	60.399	9.7 ± 1.4	0.210 ± 0.011	0.188 ± 0.014
PS70/5	14-aug-07	83.423	61.986	4.5 ± 1.0	n.m	0.180 ± 0.018
PS70/3	11-aug-07	85.145	60.815	11.2 ± 1.9	n.m	n.m
PS70/6	7-sep-07	84.499	−138.389	15.1 ± 6.0	n.m	n.m
PS70/7.1.2	8-sep-07	84.450	−147.572	2.5 ± 0.3	0.229 ± 0.014	0.22 ± 0.02
PS70/7.2.2	8-sep-07	84.450	−147.572	5.2 ± 0.7	0.246 ± 0.017	n.m
PS70/7.3.2	8-sep-07	84.450	−147.572	2.7 ± 0.9	0.226 ± 0.018	0.20 ± 0.03
PS70/8.1	17-sep-07	84.261	108.746	16.6 ± 3.8	n.m	n.m
PS70/8.2	17-sep-07	84.261	108.746	8.1 ± 0.9	n.m	n.m
PS70/8.3	17-sep-07	84.261	108.746	7.2 ± 1.5	0.233 ± 0.012	0.224 ± 0.017
PS70/9.2	17-sep-07	84.215	108.916	20.4 ± 1.1	0.329 ± 0.018	0.216 ± 0.019

(1998); Cooper et al. (1998), Masqué et al. (2003; 2007) and Cota et al. (2006). The combined dataset shall be sufficiently detailed to permit identification of areas of sea ice origin, by comparing the $^{240}Pu/^{239}Pu$ atom ratios and ^{137}Cs, $^{239,240}Pu$ concentrations in SIS with those reported in bottom sediments from the Arctic continental shelves.

The specific activities of anthropogenic radionuclides in SIS can be explained by multiple factors, including sediment source area, grain-size fractionation during sea-ice formation and addition of radionuclides to the ice from atmospheric deposition or scavenging from surrounding sea water during drift (Landa et al., 1998; Cooper et al., 2000; Baskaran, 2005). At the time of collection of the samples considered here (1998–2007), the atmospheric fluxes of ^{137}Cs and $^{240,239}Pu$ were negligible. Another process which might enhance the radionuclide concentration in SIS is the direct uptake from ice during seasonal ice melting. However, this process is also likely to be insignificant because chemical compound solutes are generally excluded from the ice during formation due to the segregation of ions from the crystal ice (Weeks and Ackley, 1986). Deposition of dust onto sea ice is generally regarded as unimportant (Pfirman et al., 1989, 1990). Hence radionuclides associated with SIS are likely to reflect dominantly the isotopic signature of sediments in source areas and thus might be used as a source signature or fingerprint of the area in which the ice incorporated its sediment.

4.1. Distribution of anthropogenic radionuclides concentrations in sea-ice sediments

The specific activities of both ^{137}Cs and $^{239,240}Pu$ in SIS in the Arctic Ocean range over four orders of magnitude, from 1.8 to $4 \cdot 10^3$ Bq kg^{-1} for ^{137}Cs and from 0.021 to 31.8 Bq kg^{-1} for $^{239,240}Pu$ (Fig. 2). The highest activities of ^{137}Cs and $^{239,240}Pu$ were measured in the same SIS sample collected from an iceberg close to Franz Josef Land. High concentrations of ^{137}Cs were also measured at Resolute Bay (Canadian archipelago) (1785 and 2094 Bq kg^{-1}), in two SIS samples collected from multi-year ice (Cota et al., 2006). However, most of the SIS samples contained less than 1.4 Bq kg^{-1} and less than 45 Bq kg^{-1} of $^{239,240}Pu$ and ^{137}Cs, respectively (Fig. 2). These values were identified as extreme-outliers values based upon box-quartile analysis, and thus they were used as criteria to identify samples with anomalously high activities.

Despite the large variation in activities of both radionuclides, three main sectors could be identified within the Arctic Ocean based on ^{137}Cs and $^{239,240}Pu$ activities: the Eurasian Basin ($n=41$), the Canadian Basin ($n=30$) and the Fram Strait ($n=31$) (Fig. 2). The largest variability for both radionuclides was found in the Eurasian Basin, where ^{137}Cs and $^{239,240}Pu$ concentrations ranged from 1.8 to $4 \cdot 10^3$ Bq kg^{-1} and from 0.02 to 31.8 Bq kg^{-1}, respectively, and also in the Fram Strait, with ^{137}Cs and $^{239,240}Pu$ ranging from 2.2 to 651 Bq kg^{-1} and 0.09 to 9.5 Bq kg^{-1}, respectively. In contrast, activities in SIS in the Canadian Basin vary relatively less than in other sectors (0.10–1.82 Bq kg^{-1} for $^{239,240}Pu$ and 1.7–73 Bq kg^{-1} for ^{137}Cs). It is interesting to notice that these three sectors mirror the main patterns described from the mean field of sea ice motion: the TPD dominates in the Eurasian Basin, the Beaufort Gyre dominates in the Canadian Basin and the Fram Strait is the principal ablation area.

Within the Eurasian Basin, the highest variability of both radionuclides was found in the Siberian sector, in the Nansen and Amundsen Basins (from 0.4 to $4 \cdot 10^3$ Bq kg^{-1} for ^{137}Cs and from 0.018 to 31.9 Bq kg^{-1} for $^{239,240}Pu$). This variability is explained by the fact that this area is a potential convergence region of sea ice originated mainly in the Russian shelves, where comparable ^{137}Cs and $^{239,240}Pu$ activities have been reported in bottom sediments (AMAP, 2002). Also, Pavlov et al. (2004), based on a sea ice drift model, identified the Kara Sea and the Novaya Zemlya archipelago as the most likely origin for sea ice surrounding Franz Joseph Land and Svalbard; this supports the comparison of ^{137}Cs and $^{239,240}Pu$ activities reported in SIS and surface sediments from the vicinity of the Novaya Zemlya archipelago (AMAP, 2002; Smith et al., 1995, 2000).

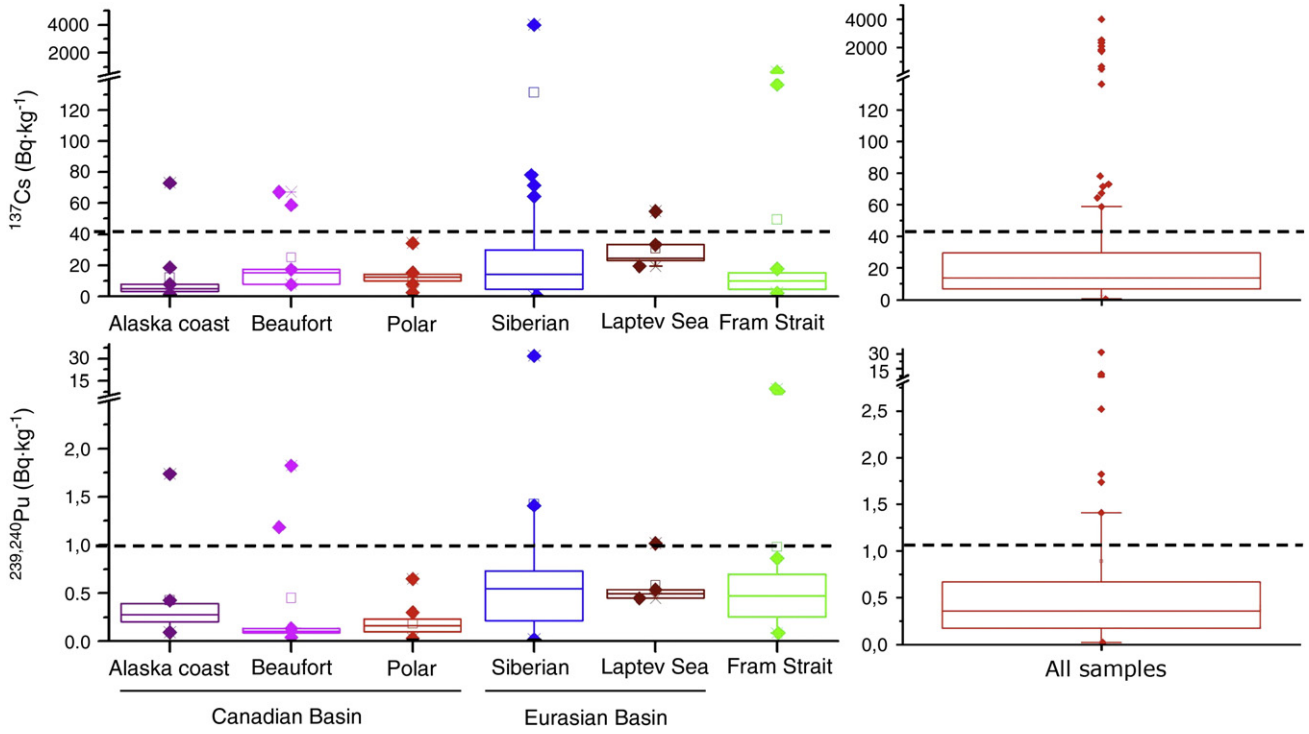

Fig. 2. Box analysis of ^{137}Cs concentrations (a) and $^{239,240}Pu$ atom ratios (b) in sea-ice sediments in the Arctic Ocean (including data from this study and from Meese et al. (1997), Landa et al. (1998), Cooper et al. (1998), Baskaran (2005), Masqué et al. (2003, 2007) and Cota et al. (2006). The median, first and third percentile, 95% percentile (vertical line), outliers (filled points), maximum and minimum values (stars) are indicated.

The Laptev Sea is an area where the highest median ^{137}Cs and ^{239,240}Pu activities in SIS were measured: 26 Bq kg^{-1} and 0.515 Bq kg^{-1}, respectively. Also, variability in concentrations is rather limited, ranging from 19.5 to 54.8 Bq kg^{-1} for ^{137}Cs and from 0.45 to 1.012 Bq kg^{-1} for ^{239,240}Pu, and compare well with reported concentrations in bottom sediments of the Laptev Sea shelf: from 0.01 to 2 Bq kg^{-1} for ^{239,240}Pu (AMAP, 2002) and from 0.86 to 16 Bq kg^{-1} for ^{137}Cs (Johnson-Pyrtle and Scott, 2001). The only other possible source area of these sea-ice sediments is the Kara Sea, reaching the area through the Vilkitsky Strait. Indeed, SIS collected from a floe in the Vilkitsky Strait had activities as high as 54.8 Bq kg^{-1} for ^{137}Cs and 1.02 Bq kg^{-1} for ^{239,240}Pu (Landa et al., 1998). Both values are comparable to those measured in bottom sediment from the Kara Sea and hence suggest that this particular ice floe incorporated the sediments in the Kara Sea.

In the Canadian Basin, a region dominated by the Beaufort Gyre, three subsectors could also be identified; the Alaskan coast ($n=9$), the Canada and Makarov Basins (identified as Beaufort in Fig. 2) ($n=8$) and the central Arctic Ocean ($n=13$) (Fig. 2). Despite the fact that ^{137}Cs and ^{239,240}Pu activities vary similarly, slight differences exist in relation to the median activities. For ^{137}Cs, the median activity in the Canada and Makarov Basins is approximately 3 times greater than that in the Alaskan continental shelves (4.9 Bq kg^{-1}). In contrast, the median ^{239,240}Pu concentration in the Canada and Makarov Basins) is more than 2 times lower than in the Alaska continental shelves (0.28 Bq kg^{-1}). These results suggest that the dominant source of sea ice is different for each of these regions. From comparison of ^{137}Cs activities in shelf-bottom sediments with those in SIS it can be inferred that sea ice in the Canada and Makarov Basins is more likely to be formed in the Siberian shelves, while sea ice in the Alaska continental shelves is formed along the Chukchi Sea and the Canadian archipelago.

Median activities of ^{137}Cs and ^{239,240}Pu in SIS from the central Arctic Basin were 12.4 and 0.16 Bq kg^{-1}, respectively, which compare well with concentrations reported in SIS from the Alaska continental shelves and the Canadian and Makarov Basins, suggesting a mixture between both areas. This is in agreement with the findings of Pfirman et al. (1997), who stated that sea ice in the central Arctic Basin is formed by ice from diverse sources, identifying Alaska, the Canadian archipelago and the East Siberian Seas as main sources of sea ice.

The distribution of sea ice in the Fram Strait is governed by the oceanographic circulation, and is formed by a mixture of sea ice floes with distinct origins because the diverse trajectories for sea ice drift merge here. This fact is reflected in a large degree of variability in ^{137}Cs and ^{239,240}Pu activities in the Fram Strait (Fig. 2). The highest range of activities of both radionuclides, 10–652 Bq kg^{-1} for ^{137}Cs and 0.31–9.5 Bq kg^{-1} for ^{239,240}Pu, were measured along the permanent ice covered region on the western side. The East Greenland Current flows through this area, and sea ice could have been formed in the eastern Arctic continental shelves and have been driven by the TPD (Wadhams, 1983). This is in agreement with the fact that reported ^{137}Cs and ^{239,240}Pu activities in bottom sediments from the Siberian continental shelves are higher than those in the western Arctic Ocean (e.g. Baskaran et al., 1995; 2000; Huh et al., 1997; Meese et al., 1997; Smith et al., 2000; Johnson-Pyrtle and Scott, 2001; Oughton et al., 2004). ^{137}Cs and ^{239,240}Pu activities in the central-eastern side of the Fram Strait and in the Eastern Greenland continental shelves vary from 3.8 to 23 Bq kg^{-1} and from 0.018 to 0.71 Bq kg^{-1}, respectively. However, SIS samples from the Eastern Greenland area consisted mostly of sand (70%) (data not shown), in agreement with the description of bottom sediments by Berner and Wefer (1990), who reported that sand accounts for more than 50% of the sediments in the shelf areas of Greenland. Earlier sea-ice sediment studies carried out in the central Arctic Basin and in the Eurasian shelves (e.g. Nürnberg et al., 1994; Dethleff, 2005; Eicken et al., 2005) suggested that entrained materials consist of 60–90% fine-grained (<63 mm) silt and clay, with an essentially terrestrial origin. Therefore, the presence of either high or low concentrations of ^{137}Cs and ^{239,240}Pu associated with low fine-grained content must be driven by the transport of particulate matter for long distances across the Arctic Ocean and not from Greenland.

Overall, and despite the large variability of ^{137}Cs and ^{239,240}Pu activities in SIS along the Arctic Ocean, a reasonable correlation exists between both radionuclides ($R^2=0.82$, Fig. 3). As a general trend, most SIS samples contain ^{137}Cs and ^{239,240}Pu in similar proportions, with a median ^{239,240}Pu/^{137}Cs ratio of $32\cdot10^{-3}$. This suggests that the ultimate source of most ^{239,240}Pu and ^{137}Cs in the SIS, and therefore in the bottom sediments mostly delivered by rivers of continental shelves, is the same around the Arctic Ocean. In fact, the median ^{239,240}Pu/^{137}Cs ratio is in good agreement with the global fallout value, $\sim34\cdot10^{-3}$ in 2007, based upon decay correction of data in Beck and Krey (1983). This conclusion is reasonable because global fallout is regarded as the main source of both radionuclides to the Arctic Ocean (JRNEG, 1996, Oughton et al. 1999). However, it is necessary to use caution when using the ratio to attribute the source of ^{137}Cs and ^{239,240}Pu to global fallout. The ^{239,240}Pu/^{137}Cs ratio in bottom sediments depends on many factors: decay, scavenging of the radionuclides by particles during sedimentation, water column depth and proximity to river outflows, sediment characteristic and composition or radionuclide chemical features. In particular the distribution coefficients (K_d) for Pu and Cs in the marine environment are significantly different ($1\cdot10^5$ and $2\cdot10^3$, respectively; IAEA, 1985), as Pu is more particle reactive than ^{137}Cs.

In spite of the good general correlation between ^{137}Cs and ^{239,240}Pu concentrations, slight differences were observed, suggesting that SIS were imprinted by secondary sources in addition to global fallout (Fig. 3). This is markedly the case for samples considered as anomalous based on the criteria of higher activities (>45 Bq kg^{-1} for ^{137}Cs and >1.4 Bq kg^{-1} for ^{239,240}Pu).

4.2. Distribution of ^{240}Pu/^{239}Pu atom ratios in sea-ice sediments

The ^{240}Pu/^{239}Pu atom ratio can be used to identify local sources of Pu other than global fallout. Although the main source of Pu isotopes to the Arctic Ocean is global fallout from the nuclear weapons testing (Oughton et al., 2004; Skipperud et al., 2004), additional local and regional sources, including local fallout from tropospheric weapons testing, dumping of nuclear waste, marine and terrestrial transport from the reprocessing plants, and input from nuclear accidents that occurred in proximity to the Arctic Ocean (Tomsk-7) have all contributed to enhancing ^{239,240}Pu and ^{137}Cs activities and modifying the ^{240}Pu/^{239}Pu atom ratios in specific areas of the Siberian shelves (Cochran et al., 2000). In general, the ^{240}Pu/^{239}Pu atom ratio is relatively uniform in the bottom sediments along the continental shelves of the Arctic Ocean (Skipperud et al., 2004) and is comparable to the characteristic ratio of global fallout, (0.183 ± 0.009). However, low ^{240}Pu/^{239}Pu atom ratios have been reported in bottom sediments from areas such as Kara Sea and Novaya Zemlya archipelago, ranging from 0.03 at Chernaya Bay to 0.16 ± 0.03 at the Kara Gate (Smith et al., 2000; Oughton et al., 2004). On the other hand, ratios slightly higher than the global fallout (0.1939 ± 0.0013), were measured in sediments at Point Barrow, Alaska (Kelley et al., 1999).

Huh et al. (1997) suggested that ^{240}Pu/^{239}Pu atom ratios in sediment cores from the deep Arctic Basin correspond to a mixture of global fallout inputs, which decreases with increasing latitudes, and discharges from reprocessing plants in Russia and in the Atlantic area. Cooper et al. (2000) suggested that Pu associated with SIS can be considered as a source of Pu to the bottom sediments, although the total flux of Pu from SIS to the deep sea would be relatively small. Recent studies of ^{240}Pu/^{239}Pu atom ratios in bottom sediments in the Fram Strait have provided evidence of the long distance dispersion of Pu in the Arctic Ocean associated to sea-ice sediments (Masqué et al., 2003). This demonstrates that sea-ice is an efficient transport agent of

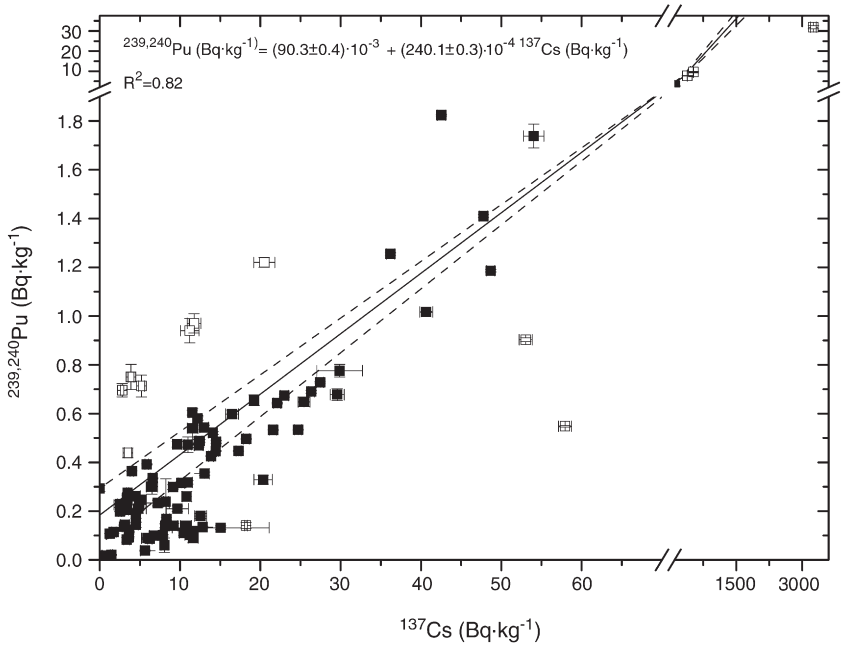

Fig. 3. Relationship between all ^{239,240}Pu vs ^{137}Cs activities in sea-ice sediments from the Arctic Ocean (including data from this study and from Meese et al. (1997), Landa et al. (1998), Cooper et al. (1998), Masqué et al. (2003, 2007). Confidence intervals at 95% are shown ($R^2 = 0.82$). Red points are considered as outliers and are not included into the regression.

Pu associated with sediments and the fate of sea ice and associated radionuclides to sea-ice sediments is closely coupled.

The ^{240}Pu/^{239}Pu atom ratios in SIS are generally comparable to that of global fallout (0.18, JRNEG, 1996; Krey et al., 1976). This is expected because most of the continental shelves have been affected by Pu derived from global fallout (Fig. 4). Deviations from it have been observed at the Fram Strait (0.14 – 0.21) and the Eurasian Basin (0.12–0.22) due to the fact that the former area is the region where all drift pathways merge while the latter is influenced by the extensive source areas of the Siberian shelves (Nürnberg et al., 1994; Eicken et al., 1997). In the western Arctic Ocean, in contrast, ^{240}Pu/^{239}Pu atom ratios range from 0.17 to 0.19, showing clearly the signature of global fallout. However, the exceptions to this trend are two samples, 218-1 and 234-1, collected close to the North Pole. These samples likely originated in the vicinity of the Kara Sea, as inferred from their lower ^{240}Pu/^{239}Pu atom ratios. The ice floes carrying these SIS could reach

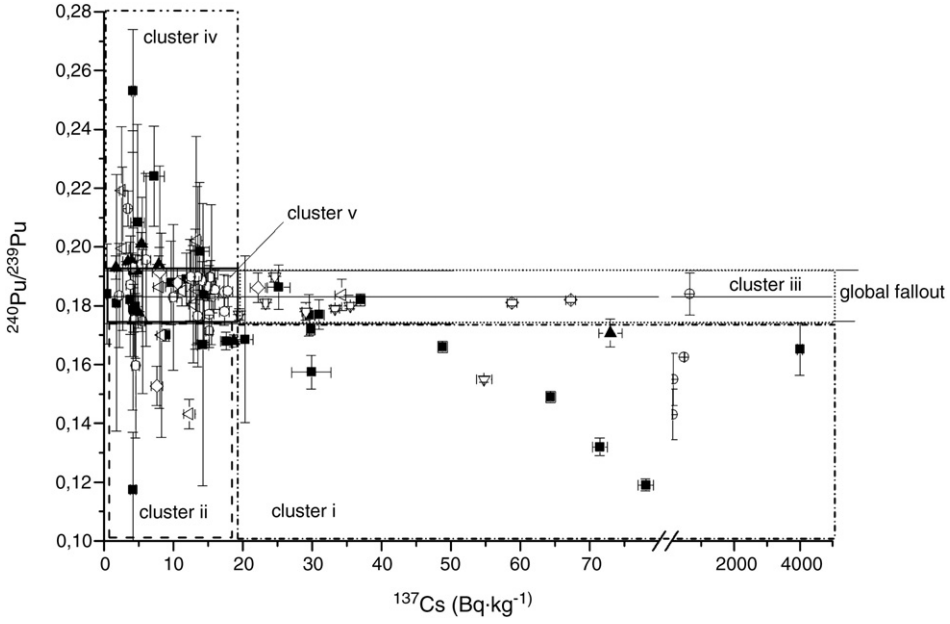

Fig. 4. Relationship of all available data of ^{137}Cs activities vs ^{240}Pu/^{239}Pu atom ratios in sea-ice sediments collected in the Arctic Ocean including data from this study and from Meese et al. (1997), Landa et al. (1998), Cooper et al. (1998) and Masqué et al. (2003, 2007). Samples are divided according to the mean sea ice drift patterns: Fram Strait (circles), Siberian (solid squares), Laptev Sea (reversed triangle), Polar-central Arctic (triangle), Beaufort (rhombus) and Alaska continental shelves (solid triangle). Five clusters are identified using a ^{240}Pu/^{239}Pu atom ratio of 0.183 ± 0.009 and a ^{137}Cs activity of 20 Bq kg^{-1} as limits. These clusters are used to hypothesized source areas for sea-ice sediments (see text for details).

the western Arctic as a result of exchange between TPD and Beaufort Gyre. Also, $^{240}Pu/^{239}Pu$ atom ratios slightly higher than global fallout were found in SIS in the Alaska coast (Landa et al., 1998). Those are comparable to $^{240}Pu/^{239}Pu$ atom ratios determined in the sediments of Point Barrow, suggesting that their origin was close to the site of sampling.

4.3. Linking radionuclide signatures of SIS to areas of sea ice origin

As shown in Fig. 4 and noted above, most SIS samples have $^{240}Pu/^{239}Pu$ atom ratios comparable to that of stratospheric bomb fallout (0.183 ± 0.009), irrespectively of their ^{137}Cs concentrations. In particular, samples with elevated ^{137}Cs concentrations are not necessarily characterized by non-global fallout Pu atom ratios, implying that ^{137}Cs alone cannot be used to identify an origin area of sea ice. The combination of both datasets may allow us to identify source areas of the SIS and thus of sea ice. Several clusters of radionuclide signature can be identified according to two criteria (Fig. 4): deviations of the $^{240}Pu/^{239}Pu$ atom ratios relative to the global fallout value (0.183 ± 0.009) and ^{137}Cs activities higher or lower than 20 Bq kg^{-1}, as it has been reported that concentrations of ^{137}Cs originated from global fallout in most continental shelf sediments are <20 Bq kg^{-1} (AMAP, 2002). These clusters include: i) samples with $^{240}Pu/^{239}Pu$ atom ratios <0.174 and ^{137}Cs activities >20 Bq kg^{-1}; ii) samples with $^{240}Pu/^{239}Pu$ atom ratios lower than 0.174 and ^{137}Cs activity <20 Bq kg^{-1}; iii) samples with $^{240}Pu/^{239}Pu$ atom ratios within the range of global fallout and ^{137}Cs activities >20 Bq kg^{-1}; iv) samples with $^{240}Pu/^{239}Pu$ atom ratio greater than global fallout but with low ^{137}Cs activities (<20 Bq kg^{-1}) and v) samples with $^{240}Pu/^{239}Pu$ atom ratio comparable to the global fallout and ^{137}Cs activities <20 Bq kg^{-1}.

4.3.1. Kara Sea

As shown in Fig. 4, cluster (i) (short dash-dots line), a group of SIS samples is characterised by $^{240}Pu/^{239}Pu$ atom ratios lower than the global fallout value (<0.174) and ^{137}Cs activities greater than 20 Bq kg^{-1}. Low $^{239}Pu/^{240}Pu$ atom ratios correspond to a mixture between global fallout and low-yield nuclear testing fallout or material released from nuclear reprocessing plants. Among the Arctic continental shelves, low $^{240}Pu/^{239}Pu$ atom ratios have been reported only in the Kara Sea and the Novaya Zemlya archipelago, as a result of local fallout, discharge from rivers and nuclear waste dumping (Smith et al., 2000; Skipperud et al., 2004). ^{137}Cs and $^{239,240}Pu$ activities in SIS are greater than those typical for continental shelf sediment affected by global fallout (20 Bq kg^{-1} for ^{137}Cs and 1 Bq kg^{-1} for $^{239,240}Pu$; Smith et al., 2000). Previous studies have reported elevated activities of ^{137}Cs and $^{239,240}Pu$ (>45 Bq kg^{-1} and >1 Bq kg^{-1}, respectively) in bottom sediments of the Kara Sea (AMAP, 1998; Baskaran et al., 1995; Smith et al., 2000), and thus this could be a likely origin area for SIS with low $^{239}Pu/^{240}Pu$ atom ratios and high ^{137}Cs and $^{239,240}Pu$ activities. The SIS samples showing these isotopic signatures were collected in the west side of the Fram Strait and in the Siberian Branch of the TPD, regions that are principally within the drift path for sea ice formed along the western Arctic shelves, particularly between the Laptev Sea and the Novaya Zemlya Archipelago (Pfirman et al., 2004; Wadhams, 1983).

Another group of samples are characterized by low Pu atom ratios (<0.174) but also low ^{137}Cs specific activities (<20 Bq kg^{-1}), cluster (ii) (Fig. 4, dash line). Given the low $^{240}Pu/^{239}Pu$ atom ratios of these samples, the most probable source area would also be the Kara Sea and its surrounding areas. The low ^{137}Cs specific activities are likely due to the other factors that affect specific activity (described in Section 4.1), and in any case are within the range of activities found in surface bottom sediments (2-33 ^{137}Cs Bq kg^{-1}, Livingston and Povinec, 2000). This reinforces the concept that the $^{240}Pu/^{239}Pu$ atom ratio is a better indicator of SIS source than the ^{137}Cs specific activity.

4.3.2. Laptev–Kara Sea

A number of SIS samples display $^{240}Pu/^{239}Pu$ atom ratios typical of global fallout and high ^{137}Cs activities (>20 Bq kg^{-1}), cluster (iii) (Fig. 4, dot line). The $^{240}Pu/^{239}Pu$ atom ratios suggest that any continental shelf area might be the origin of the sediments. High ^{137}Cs activities were measured in bottom sediments in the western Kara and Laptev Seas (AMAP, 1998; Baskaran et al., 1995; Smith et al., 2000, personal communication by A. Johnson-Pyrle in Meese et al., 1997), although elevated inventories of ^{137}Cs in bottom sediments could result from a combination of processes related to the sedimentation dynamics, Johnson-Pyrtle and Scott (2001) hypothesized that elevated ^{137}Cs inventories in bottom sediments may be the result of ^{137}Cs origin other than direct atmospheric fallout, indicating the Lena river as a secondary source. In the absence of any other direct source of ^{137}Cs in its drainage basin, it is likely that ^{137}Cs introduced into the Lena river comes from the erosion of global fallout and possibly from Chernobyl derived contamination.

Several SIS samples with these characteristics were collected in the Laptev Sea and along the northwest of Franz Josep Land. The Franz Josef Land is within the Siberian Branch of the TPD. Prior studies have considered the Laptev Sea as the major source of sea ice to the Siberian Branch of the TPD, with the Kara Sea as a secondary source (Nürnberg et al., 1994; Pfirman et al., 1997).

Back trajectory analysis of three samples (sample coded PS93-235-1-2; Landa et al., 1998 and 212-2 and 218-1; Cooper et al., 2000) collected in the western part of the Arctic Ocean suggested that they originated from the Canadian archipelago and the Beaufort Sea (Tucker et al., 1999). However, the ^{137}Cs and $^{240,239}Pu$ activities and $^{240}Pu/^{239}Pu$ atom ratios of these samples argue against these areas as the origin, as no elevated ^{137}Cs and $^{239,240}Pu$ concentrations have been reported in North American continental shelves (Meese et al., 1997; Landa et al., 1998). It is more likely that these sediments originated and were incorporated into sea ice in the Laptev Sea, and reached the western basin by exchange between the TPD and the Beaufort Gyre. The most likely scenario for the transport of Laptev Sea-derived SIS into the Beaufort Gyre occurs when a positive Arctic Oscillation (AO), which favours strong advection of ice away from the Siberian shelves into the central Arctic, is followed by negative AO conditions, increasing the size of the Beaufort Gyre and capturing sea ice into the Beaufort Gyre. The three samples from the western part of the Arctic Ocean were collected in 1994 (Cooper et al., 1998). The years immediately preceding the sampling activities (1989 to 1995) were mostly years of a + AO (Mysak, 2001), supporting the hypothesis that they could have originated in the Laptev Sea. During these years, the TPD would be strengthened and pushed closer to Beaufort Sea, making the transport of Laptev Sea into the Beaufort Gyre more likely.

4.3.3. North American shelves

Most of the samples collected in the western part of the Arctic Ocean close to the Alaska coast, as well as samples collected on the western side of the Fram Strait form another cluster with $^{240}Pu/^{239}Pu$ atom ratios greater than global fallout (0.19–0.25) and ^{137}Cs activities mostly below 10 Bq kg^{-1}, cluster (iv) (Fig. 4, dash-dot line). North American shelves are likely the origin area for such SIS: relatively elevated $^{240}Pu/^{239}Pu$ atom ratios were measured in bottom sediments from Point Barrow (Kelley et al., 1999), while average activities of ^{137}Cs in surface bottom sediments in the Bering and Chukchi Seas and in the East Chukchi Sea are low (4.2 ± 2.8 Bq kg^{-1}, Meese et al. (1997) and 2.9 ± 0.7 Bq kg^{-1}, Baskaran and Naidu (1995), respectively). The high $^{240}Pu/^{239}Pu$ atom ratios in samples from the western Fram Strait highlight the importance of long-distance transport SIS from the Beaufort Sea across the Arctic Ocean. These sea ice floes and their contained SIS would have originated in the shallow parts of the

Beaufort and Chukchi Seas, close to the shore, and drifted eastward, traversing the Arctic Ocean via the Beaufort Gyre and being captured by the Polar Branch of the TPD before finally reaching the Fram Strait. Indeed, this is supported by Pfirman et al. (1997), that concluded that North American shelves were the origin for sea ice that flows into western Arctic Ocean and the western part of the Fram Strait.

4.3.4. Unidentifiable source areas

Approximately 50% of the analysed samples have $^{240}Pu/^{239}Pu$ atom ratios comparable to that of global fallout and ^{137}Cs specific activities lower than $<20\ Bq\ kg^{-1}$, cluster (v), (Fig. 4, solid line). The anthropogenic radionuclide distributions in most of the continental shelves of the Arctic Ocean are typical of global fallout origin, and thus the isotopic signature is not distinct as to identify the source areas of SIS. Additional analyses, such as Fe oxide mineral grains (Darby, 2003), planktonic diatom species (Abelmann, 1992), or smectite and illite analysis (Wollenburg, 1993; Dethleff et al., 1993; Nürnberg et al., 1994) may help to constrain more accurately the origin of these samples.

5. Conclusions

Based on a combined dataset of previously published and new analyses of ^{137}Cs and $^{239,240}Pu$ and the $^{240}Pu/^{239}Pu$ atom ratios in Arctic sea-ice sediments (SIS), we conclude that these anthropogenic radionuclides can be used in many instances to determine the geographical source area in which the sediments were incorporated into the ice. This information, in addition, can be used to elucidate the sea ice floes formation areas. The $^{240}Pu/^{239}Pu$ atom ratio, in combination with the ^{137}Cs or $^{239,240}Pu$ activity, is especially useful in this regard. SIS originating in the Laptev and Kara Seas have $^{240}Pu/^{239}Pu$ atom ratios lower than those imprinted by global fallout (<0.18), while SIS originating from the Alaskan shelf is characterised by $^{240}Pu/^{239}Pu$ atom ratios greater than global fallout. The specific activities of ^{137}Cs and $^{239,240}Pu$ are less diagnostic of sea-ice origin, because many processes in addition to source can affect their values; however, sediments of the Kara and Laptev Seas can have markedly elevated specific activities of ^{137}Cs that are imprinted on SIS originating in those areas. In approximately 50% of the samples analyzed, the isotopic signatures are not distinctive as to SIS origin and additional approaches are required to better resolve possible source areas.

Acknowledgements

This work was partially funded by the Ministerio de Eduación y Ciencia of Spain (POL2006-00449). The US National Science Foundation supported portions of this study. The first author expresses her gratitude to MEC through her scholarship AP2006-03071. Support for the research of PM was received through the prize ICREA Academia, funded by the Generalitat de Catalunya. Support from the government of Spain and the Fulbright Commission for a post-doctoral fellowship to J.G.-O. (ref 2007-0516) is gratefully acknowledged. We are thankful to the crew and technicians of the R/V Polarstern for assistance during ARK XXII/2 and to V. Shevchenko, C. Kierdoff and J. Mathiessen for collecting and providing us sea-ice sediments samples. This is contribution No. 1394 from the School of Marine and Atmospheric Sciences.

References

Aarkrog A. Input of anthropogenic radionuclides into the World Ocean. Deep-Sea Res II 2003;50(17–21):2597–606.
Abelmann A. Diatom assemblages in Arctic sea ice-indicator for ice drift pathways. Deep-Sea Res 1992;39(Suppl2):S525–38.
AMAP. Arctic pollution issues: a state of the arctic environment report. Arctic Monitoring and Assessment Programme; 1998.
AMAP. Arctic Pollution Issues: A State of the Arctic Environment Report. Arctic Monitoring and Assessment Programme. AMAP Assessment 2002: Radioactivity in the Arctic; 2002.
Baskaran M. Interaction of sea ice sediments and surface sea water in the Arctic Ocean: evidence from excess ^{210}Pb. Geophys Res Lett 2005;32:LI2601. doi:10.1029/2004GL022191.
Baskaran M, Naidu J. ^{210}Pb-derived chronology and the fluxes of ^{210}Pb and ^{137}Cs isotopes into continental shelf sediments, East Chukchi Sea, Alaska Arctic. Geochim Cosmochim Acta 1995;59:4435–48.
Baskaran M, Asbill S, Santschi P, Davis T, Brooks J, Champ M, et al. Distribution of Pu-230, Pu-240 and Pu-238 concentrations in sediments from the Ob and Yenisey rivers and the Kara Sea. Appl Radiat Isot 1995;46:1109–19.
Baskaran M, Shaunna A, Santschi P, Brooks J, Champ M, Adkinson D, et al. Pu, ^{137}Cs and excess ^{210}Pb in the Russian Arctic sediments. Earth Planet Sci Lett 1996;140:243–57.
Baskaran M, Asbill S, Schwantes J, Santschi PH, Champ MA, Brooks JM, Adkinson D, Makeyev V. Concentrations of 137Cs, 239, 240Pu, and 210Pb in sediment samples from the Pechora Sea and biological samples from the Ob, Yenisey Rivers and Kara Sea. Mar Pollut Bull 2000;40:830–8.
Baxter MS, Fowler SW, Povinec PP. Observations on plutonium in the oceans. Appl Radiat Isot 1995;46(11):1213–23.
Beck HL, Krey PW. Radiation exposure in Utah from Nevada Nuclear Tests. Science 1983;220:18–24.
Berner H, Wefer G. Physiographic and biological factors controlling surface sediment distribution in the Fram Strait. In: Bleil U, Thiede J, editors. Geological history of the Polar Oceans: Arctic versus Antartic. Dordrecht: Klower; 1990. p. 317–35.
Buesseler KO. Plutonium isotopes in the North Atantic. PhD. Thesis, Massachussets Institute of Technology/Woods Hole Oceanographic Institution Joint Program in Oceanography;1986, pp. 220.
Chamizo E, Jimenez-Ramos MC, Wacke RL, Vioque I, Calleja A, García-León M, et al. Isolation of Pu-isotopes from environmental simples using ion chromatography for accelerator mass spectrometry and alpha spectrometry. Anal Chim Acta 2008a;606:239–45.
Chamizo E, Enamorado SM, García-León M, Suter M, Wacker L. Plutonium measurements on the 1 MV compact AMS system at the Centro Nacional de Aceleradores (CNA). Nucl Instrum Meth Phys Res B 2008b;266:4948–54.
Christensen GC, Romanov GN, Strand P, Saibu B, Malyshev SV, Bergan TD, et al. Radioactive contamination in the environment of the nuclear enterprise "MAYAK" PA. Results from the joint Russian–Norwegian field work in 1994. Sci Total Environ 1997;202:237–48.
Cochran JK, Moran SB, Fisher NS, Beasley TM, Kelley JM. Sources and transport of anthropogenic radionuclides in the Ob River system, Siberia. Earth Planet Sci Lett 2000;179:125–37.
Cooper LW, Larsen IL, Beasley TM, Dolvin SS, Grebmeier JM, Kelley JM, et al. The distribution of radiocesium and plutonium in Sea Ice-entrained Arctic sediments in relation to potential sources and sinks. J Environ Radioactiv 1998;39(3):279–303.
Cooper LW, Kelley JM, Bond LA, Orlandini KA, Grebmeier JM. Sources of the transuranic elements plutonium and neptunium in arctic marine sediments. Mar Chem 2000;69:253–76.
Cota GF, Cooper LW, Darby DA, Larsen IL. Unexpectedly high radioactivity burdens in ice-rafted sediments from the Canadian Arctic Archipelago. Sci Total Environ 2006;366:253–61.
Darby DA. Sources of sediments found in sea ice from the western Arctic Ocean, new insights into processes of entrainment and drift pattern. J Geophys Res 2003;108(C8):3257.
Dethleff D. Entrainment and export of Laptev Sea ice sediments, Siberian Arctic. J Geophys Res 2005;110:C07009. doi:10.1029/2004JC002740.
Dethleff D, Nürnberg D, Gorth E. East Siberian Arctic region expedition '92: the Laptev Sea : its significance for Arctic sea-ice formation and transpolar sediment flux. Reports on Polar Research, 120. ; 1993. 44 pp.
Efurd ED, Steiner RE, Roensch FR, Glover SE, Musgrave JA. Determination of the $^{240}Pu/^{239}Pu$ atom ratio in global fallout at two locations in the Northern Hemisphere. J Radioanal Nucl Chem 2005;263(2):387–91.
Eicken H, Reimnitz E, Alexandrov V, Martin T, Kassens H, Viehoff T. Sea-ice processes in the Laptev Sea and their importance for sediment export. Cont Shelf Res 1997;17(2):205–33.
Eicken H, Gradinger R, Gaylord A, Mahoney A, Rigor I, Melling H. Sediment transport by sea ice in the Chukchi and Beaufort Seas: increasing importance due to changing ice conditions? Deep-Sea Res II 2005;52:3281–302.
Holm E. Sources and distribution of anthropogenic radionuclides in the marine environment in radioecology: lectures in Environmental Radioactivity. Worl Scientic: Singapore; 1994.
Huh C, Pisias NG, Kelley JM, Maiti TC, Grantz A. Natural radionuclides nd plutonium in sediments from the western Arctic Ocean: sedimentation rates and pathways of radionuclides. Deep-Sea Res II 1997;44(8):1725–43.
IAEA. Sediment K_d's and concentration factors for radionuclides in the marine environment. Technical Report No. 247. Vienna: International Atomic Energy Agency; 1985.
IAEA. Radiological conditions of the Western Kara Sea. Assessment of the Radiological Waste in the Arctic Seas—Report of the International Arctic Seas Assessment Project (IASAP). Radiological Assessment Reports SeriesVienna: IAEA; 1998.
Johnson-Pyrtle A, Scott M. Distribution of ^{137}Cs in the Lena River Estuary-Laptev Sea system. Mar Pollut Bull 2001;42(10):912–26.
JRNEG. Radioactive contamination at dumping sites for nuclear waste in the Kara Sea. Results from the Russian–Norwegian 1993 expedition to the Kara Sea. Joint Russian–Norwegian Expert Group for Investigation of Radioactive Contamination of the Northern Areas82-993079-3-7; 1994.

JRNEG. Dumping of radioactive waste and investigation of radioactive contamination in the Kara Sea. Results from 3 years of investigations (1992–1994) performed by the Joint Norwegian–Russian Expert Group. Joint Russian–Norwegian Expert Group for Investigation of Radioactive Contamination of the Northern Areas82-993079-4-5; 1996.

Kabakchi SA, Putilov AV, Nazin ER. Data analysis and physicochemical modelling of the radiation accident in the southern Urals in 1957. Atomnaya Energiya 1995;78(1): 46–50.

Kelley JM, Bond LA, Beasley TM. Global distribution of Pu isotopes and ^{237}Np. Sci Total Environ 1999;237/238:483–500.

Kenna T. Determination of plutonium isotopes and neptunium-237 in environmental samples by inductively coupled plasma mass spectrometry with total sample dissolution. J Anal Atom Spectrom 2002;17:1471–9.

Krey PW, Hardy EP, Pachucki C, Rourke F, Coluzza J, Benson WK. Mass isotopic composition of global fallout plutonium in soil. Transuranium Nuclides in the EnvironmentIAEA (Internal Atomic Energy Agency), Vienna IAEA-SM-199/39; 1976. p. 671–8.

Landa E, Reimnitz E, Beals D, Pochkowski J, Rigor I. Transport of 137Cs and 239, 240Pu with ice-rafted debris in the Arctic Ocean. Arctic 1998;51:27–39.

Livingston HD, Bowen VT. Pu and ^{137}Cs in coastal sediments. Earth Plane Sci Lett 1979;43:29–45.

Livingston HD, Povinec PP. Anthropogenic marine radioactivity. Ocean Coast Manage 2000;43:689–712.

Macdonald RW, Harner TT, Fyfe J. Recent climate change in the Arctic and its impact on contaminant pathways and interpretation of temporal trend data. Sci Total Environ 2005;342:5-86.

Masqué P, Cochran JK, Hebbeln D, Hirschberg DJ, Dethleff D, Winkler A. The role of sea ice in the fate of contaminants in the Arctic Ocean: Plutonium atom ratios in the Fram Strait. Environ Sci Technol 2003;37:4848–64.

Masqué P, Cochran JK, Hirschberg DJ, Dethleff D, Hebbeln D, Winkler A, et al. Radionuclides in Arctic sea ice: tracers of sources, fates and ice transit time scales. Deep-Sea Res 2007. doi:10.1016/j.dsr.2007.04.016.

Meese DA, Reimnitz E, Tucker WB, Gow AJ, Bischof J, Darby D. Evidence for radionuclide transport by sea-ice. Sci Total Environ 1997;202:267–78.

Mysak LA. Patterns of Arctic circulation. Science 2001;293:1269–70.

Nürnberg D, Wollenburg I, Dethleff D, Eicken H, Kassens H, Letzig T, et al. Sediments in Arctic Sea ice: implications for entrainment, transport and release. Mar Geol 1994;119:185–214.

Oughton DH, Fified LK, Day JP, Cresswell RC, Skipperud L, Salbu B. Determination ^{240}Pu/^{239}Pu isotope ratio in Kara Sea and Novaya Zemlya sediments using Accelerator Mass Spectrometry. Symposium on Marine Pollution. IAEA-SM-354, IAEA, Vienna; 1999. p. 123–8.

Oughton DH, Skipperud L, Fifield LK, Cresswell RG, Salbu B, Day P. Accelerator mass spectrometry measurement of ^{240}Pu/^{239}Pu isotope ratios in Novaya Zemlya and Kara Sea sediments. Appl Radiat Isot. 2004;61:249–53.

Pavlov V, Pavlova O, Korsner R. Sea ice fluxes and drift trajectories from potential sources, computed with a statistical se ice model of the Arctic Ocean. J Mar Syst 2004;48:133–57.

Pfirman SL, Gascard JC, Wollenburg I, Mudie P, Abelmann A. Particle-laden Euroasian Arctic sea ice: observations from July to August 1987. Polar Res 1989;7:59–66.

Pfirman SL, Kogeler JW, Rigor I. Potential for rapid transport of contaminants from the Kara Sea. Sci Total Environ 1997;202:111–22.

Pfirman SL, Lange MA, Wollenburg I, Schlosser P. Sea ice characteistics and the role of sediment inclusions in deep-sea deposition: Arctic-Antarctic comparisons. In: Bleil U, Thiede J, editors. Geological Hystory of the Polar Oceans: Arctic Versus Antarctic. Kluwer Acad., Norwell, Mass; 1990. pp. 187–211.

Pfirman SL, Colony RI, Rigor I. Variability in Arctic sea ice drift. Geographr. Res. Lett. 2004;31. doi:10.1029/2004GL020063.

Rigor IG, Wallace JM, Colony R. Response of sea ice to the Arctic Oscillation. J Climate 2002;15:2648–63.

Salbu B. Actinides associated with particles. In: Kudo A, editor. Plutonium in the environment. Elsevier Science Ltd; 2001.

Skipperud L, Oughton DH, Fifield LK, Lind OC, Tims S, Brown J, et al. Plutonium isotope ratios in the Yenisey and Ob estuaries. Appl Radiat Isot 2004;60(2–4):589–93.

Smith JN, Ellis KM, Dahle S, Matishov D. Sedimentation and mixing rates of radionuclides in the Barents Sea sediments off Novaya Zemlya. Deep-Sea Res II 1995;42:1341–493.

Smith JN, Ellis KM, Polyak L, Ivanov G, Forman SL, Moran SB, et al. ^{239,240}Pu transport into the Arctic Ocean from underwater nuclear tests in Chernaya Bay, Novaya Zemlya. Cont Shelf Res 2000;20:255–79.

Thorndike V.T. Kinematics of sea ice. In: Untersteiner, N., New York, Ed. Air-Sea-Ice Interactions. Plenum Press; 1986.

Thorndike VT, Colony RI. Sea ice motion in response to geostrophic winds. J Geophys Res 1982;87:5845–52.

Tucker III WB, Gow AJ, Meese DA, Bosworth HW, Reimnitz E. Physical characteristics of summer sea ice across the Arctic Ocean. J Geophys Res 1999;104(C1):1489–504.

Vakulovsky SM, Kryshev II, Nikitin AI, Savitsky TV. and Tertyhnik EG.Radioactive contamination in the Yenisey River. J Environ Radioact 1995;29(3):225–36.

Vorobiova MI, Degteva MO, Burmistrov DS, Safronova NG, Kozheurov VP, Anspaugh LR, et al. Review of historical monitoring data on Techa River contamination. Health Phys 1999;76(6):605–18.

Wadhams P. Arctic sea-ice morphology and its measurements. J Soc Underw Technol 1983;9(2):1-12.

Waters RD, Compton KL, Noikov V, Parker FL. Releases of radionuclides to surface waters at Krasnoyarsk-26 and Tomsk-7. Report: International Institute for Applied Systems Analysis, Laxenburg, Austria; 1999.

Weeks WF, Ackley SF. The growth, structure, and properties of sea ice. In: Untersteiner N, editor. Geophysics of Sea Ice. NATO ASI Series B, PhysicsPlenum Press; 1986. p. 9-164.

Wollenburg I. Sediment transport by sea ice: the recent sediment load of lithogenic and biogenic material. Ber Polarforsschung 1993;127:1-159.

Yablokov AV, Karasev BK, Rumyatsev VM, Kokeyev ME, Petrov OI, Lystsov BN, Yemelyanenkov AF, Rubossov PM. “White bok”. Facts and problems related to radioactive waste disposal in seas adjacent to the territory of the Russian Federation. Moscow: Office of the President of the Russian Federation; 1993.